Positioning of the Mitotic Spindle by a Cortical-Microtubule Capture Mechanism

Laifong Lee,[1,2] Jennifer S. Tirnauer,[1] Junjun Li,[1] Scott C. Schuyler,[1] Jenny Y. Liu,[1] David Pellman[1]*

Correct positioning of the mitotic spindle is critical for cell division and development. Spindle positioning involves a search-and-capture mechanism whereby dynamic microtubules find and then interact with specific sites on the submembrane cortex. Genetic, biochemical, and imaging experiments suggest a mechanism for cortical-microtubule capture. Bim1p, located at microtubule distal ends, bound Kar9p, a protein associated with the daughter cell cortex. Bim1p is the yeast ortholog of human EB1, a binding partner for the adenomatous polyposis coli tumor suppressor. EB1 family proteins may have a general role in linking the microtubule cytoskeleton to cortical polarity determinants.

It has been proposed that selective stabilization of microtubules through "capture" mechanisms mediates the formation of many microtubule structures in the cell (*1–5*). However, mechanisms for microtubule capture are not well characterized. One process thought to be driven by plus-end microtubule capture is the positioning of the mitotic spindle (*2, 4, 6*). In animal cells, the position of the spindle determines the plane of cleavage, and regulated spindle rotations in specific cells give rise to asymmetric cell divisions (*2, 3*). In yeast, the axis of division is predetermined by the budding pattern, and the spindle must be aligned with the polarity of the cell for proper nuclear segregation (*6–8*).

Spindle positioning in diverse organisms has some common molecular requirements: microtubules, actin, and the dynein/dynactin complex (*6, 9, 10*). Spindle positioning is therefore one example of several important processes that are dependent on interactions between actin and microtubules (*9*). In budding yeast, dynein and dynactin are required to insert the spindle across the bud neck during anaphase but are not clearly localized to the cell cortex (*8*). Although dynein and dynactin are required for spindle positioning, and in some cells are observed at potential capture sites (*11, 12*), a direct role in plus-end microtubule capture has not been demonstrated [reviewed in (*13*)].

A second potential mechanism for spindle positioning, which is redundant with the dynein/dynactin complex, was recently identified in budding yeast (*14–17*). This genetically defined "pathway" requires the kinesin Kip3p, the formin Bni1p, and the cortical protein Kar9p. This "Kip3p pathway" is an attractive system for studying interactions of microtubules with the cell cortex, because several of its components localize to the cell cortex and are functionally linked to actin (*17–19*). Both Bni1p and actin are required for Kar9p localization to the bud cortex, explaining, at least in part, the actin requirement in spindle positioning (*20*). The cortical localization of Kar9p is particularly notable because it frequently intersects the ends of astral microtubules (*19*).

We report that Kar9p is linked to microtubules through the yeast EB1 family member Bim1p. Bim1p localized to microtubules at or near their plus ends (*21*), whereas Kar9p localized to a highly mobile cortical dot in the bud (*19, 22*). Moreover, Bim1p was required for Kar9p to interact with microtubules in vivo and in vitro.

Because mutant *bim1*Δ cells have a similar defect in orienting preanaphase spindles as do *bni1*Δ, *kar9*Δ or *kip3*Δ mutant cells (*21*), genetic crosses were used to determine if Bim1p was in the Kip3p pathway. The characteristics of Kip3p pathway defects are that cells lacking one or more Kip3p pathway genes are viable, but are inviable if they also lack dynein or dynactin genes. *bim1*Δ *kar9*Δ double mutant strains grew as well as single mutant strains at all temperatures and were no more sensitive to the microtubule-depolymerizing drug benomyl than were single mutant strains. In contrast, *bim1*Δ *dyn1*Δ strains were not viable (*23*). This suggests that Bim1p is in the Kip3p pathway.

Bim1p at wild-type levels (*21*) and overexpressed Kar9p (*19*) have partially overlapping intracellular distributions. Like the overexpressed fusion protein composed of green fluorescent protein (GFP) and Kar9p (GFP-Kar9p), GFP-Kar9p at wild-type levels localized along the length of astral microtubules and as a dot at the bud cortex that was frequently at the ends of astral microtubules (Fig. 1).

Because of their genetic interactions and partially overlapping localization, we tested if Kar9p required Bim1p to interact with microtubules. In wild-type preanaphase cells from both cycling and hydroxyurea (HU)–arrested cultures, the ends of astral microtubules intersected cortical GFP-Kar9p in more than 90% of cells (Fig. 2). In contrast, astral microtubule intersection with GFP-Kar9p was substantially reduced in *bim1*Δ cells (Fig. 2). In mating cells where GFP-Kar9p is localized at the tip of the mating projection, the interaction of microtubule ends with cortical Kar9p is also important for the process of karyogamy (*19*). In cells arrested with mating pheromone (α factor), Bim1p was required for astral microtubule ends to interact normally with GFP-Kar9p (Fig. 2).

GFP-Kar9p localization along the length of astral microtubules also required Bim1p. In contrast to wild-type cells, the GFP-Kar9p signal on astral microtubules was abolished in cells lacking Bim1p (Fig. 2). None of the preanaphase cycling cells and only 2% of preanaphase HU-arrested cells showed GFP-Kar9p along the length of astral microtubules. Similarly, GFP-Kar9p was not observed on microtubules in α factor–arrested *bim1*Δ cells. Therefore, without Bim1p, Kar9p could not bind microtubules in vivo, even when it was overexpressed (Fig. 2).

In yeast extracts, GFP-Kar9p coimmunoprecipitated with epitope-tagged Bim1p [hemagglutinin (HA)–Bim1p], and HA-Bim1p coimmunoprecipitated with GFP-Kar9p. Tubulin was not detected in the immunoprecipitates, suggesting that the Bim1p-Kar9p interaction was independent of microtubules (Fig. 3A). Bim1p also did not coimmunoprecipitate the dynactin component Nip100p (*23*). Finally,

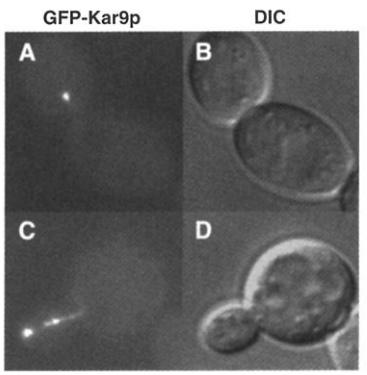

Fig. 1. GFP-Kar9p localization at wild-type levels. Fluorescent images of GFP-Kar9p are on the left and corresponding DIC (differential interference contrast) images are on the right. (**A** and **B**) GFP-Kar9p cortical dot in the bud. (**C** and **D**) GFP-Kar9p at the end and along the length of an astral microtubule. Of 150 cells analyzed for the pattern of GFP-Kar9p localization, 55% showed GFP-Kar9p localized along astral microtubules, 19% showed a cytoplasmic dot in the mother cell, and 11% showed a cortical dot in the bud. GFP-Kar9p was also observed at the centrosome and septum when overexpressed (*23*).

[1]Departments of Pediatric Oncology, The Dana-Farber Cancer Institute, and Pediatric Hematology, The Children's Hospital, Harvard Medical School, 44 Binney Street, Boston, MA 02115, USA. [2]Department of Molecular Biology, Princeton University, Princeton, NJ 08544, USA.

*To whom correspondence should be addressed. E-mail: david_pellman@dfci.harvard.edu

subpopulations of both HA-Bim1p and GFP-Kar9p cofractionated in velocity sedimentation and size-exclusion chromatography experiments. Based on the Stokes radii and Svedberg values, the estimated size of the complex is 250 kD (Fig. 3B).

To determine if Bim1p and Kar9p interacted in vitro in the absence of other yeast proteins, Kar9p and epitope-tagged Bim1p (his_7-Bim1p) were coexpressed in vitro in rabbit reticulocyte lysate. Immunoprecipitation of the translation mix with an antibody to polyhistidine demonstrated a strong interaction between his_7-Bim1p and Kar9p (Fig. 3C).

Bim1p also recruited Kar9p onto microtubules in vitro. his_7-Bim1p was purified from *Escherichia coli* and assayed for binding to polymerized microtubules. Like other EB1 family members (*24, 25*), his_7-Bim1p bound to microtubules (Fig. 4A). In vitro–translated Kar9p did not bind microtubules efficiently but did bind in the presence of his_7-Bim1p (Fig. 4, B and C). Thus, Bim1p promoted the association of Kar9p with microtubules in vitro. This interaction is specific and is unlikely to arise from "trapping" of Kar9p among bundled microtubules in the binding reaction, because Kar9p was not recruited onto microtubules by Ase1p, another yeast microtubule-binding protein with robust bundling activity (Fig. 4D).

Bim1p promotes microtubule dynamicity specifically during the G_1 phase of the cell cycle (*21*), suggesting that Bim1p is involved in the search for cortical binding sites. Here, we report that Bim1p is directly involved in the cortical capture of microtubules by its binding to Kar9p. Other likely components of this mechanism are Kip3p, Bni1p, and possibly Rho-type guanosine triphosphate-binding proteins (*18, 26*). Bim1p has also been implicated in the recently described cell-cycle checkpoint (*27*), but how it performs its checkpoint function is unknown (*28*).

A similar cortical-capture mechanism may also exist in animal cells. Bim1p is a member of the EB1 family of proteins. Like Bim1p, EB1 concentrates at microtubule plus ends (*25, 29*). EB1 interacts with the adenomatous polyposis coli (APC) tumor suppressor protein, through the region of APC that is deleted in colon cancer (*30*). APC localizes to asymmetrically distributed spots near the membrane of migrating epithelial cells (*31*). Interaction between EB1 and APC may co-

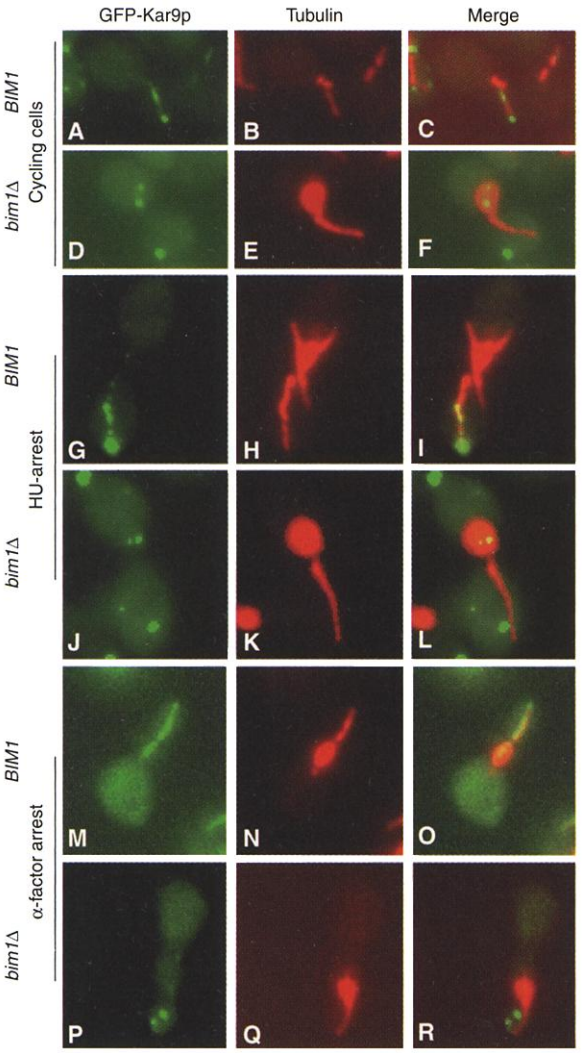

Fig. 2. Bim1p is required for GFP-Kar9p localization to microtubule ends and sides. GFP-Kar9p was expressed from a GAL1,10 promoter. GFP-Kar9p is in green (**A**, **D**, **G**, **J**, **M**, **P**), tubulin is in red (**B**, **E**, **H**, **K**, **N**, **Q**), and regions of overlap (merge column) are in yellow (**C**, **F**, **I**, **L**, **O**, **R**). Frequency of intersection of astral microtubule ends with GFP-Kar9p: 99% in preanaphase *BIM1* cells, 58% in preanaphase *bim1*Δ cells, 91% in HU-arrested *BIM1* cells, 38% in HU-arrested *bim1*Δ cells, 100% in α factor–arrested *BIM1* cells, 54% in α factor–arrested *bim1*Δ cells. To exclude *bim1*Δ cells in which the disruption of astral microtubule interaction with GFP-Kar9p was due to decreased microtubule lengths (*21, 32*) instead of a lack of Bim1p-Kar9p binding, only cells where microtubules were of sufficient length and in the correct orientation to interact with cortical Kar9p were scored (*33*). Hence, this experiment may underestimate the degree to which loss of Bim1p disrupted microtubule–GFP-Kar9p interactions in vivo. Frequency of GFP-Kar9p localization along the length of astral microtubules: 85% in preanaphase *BIM1* cells, 0% in preanaphase *bim1*Δ cells, 86% in HU-arrested *BIM1* cells, 2% in HU-arrested *bim1*Δ cells, 90% in α factor–arrested *BIM1* cells, and 0% in α factor–arrested *bim1*Δ cells.

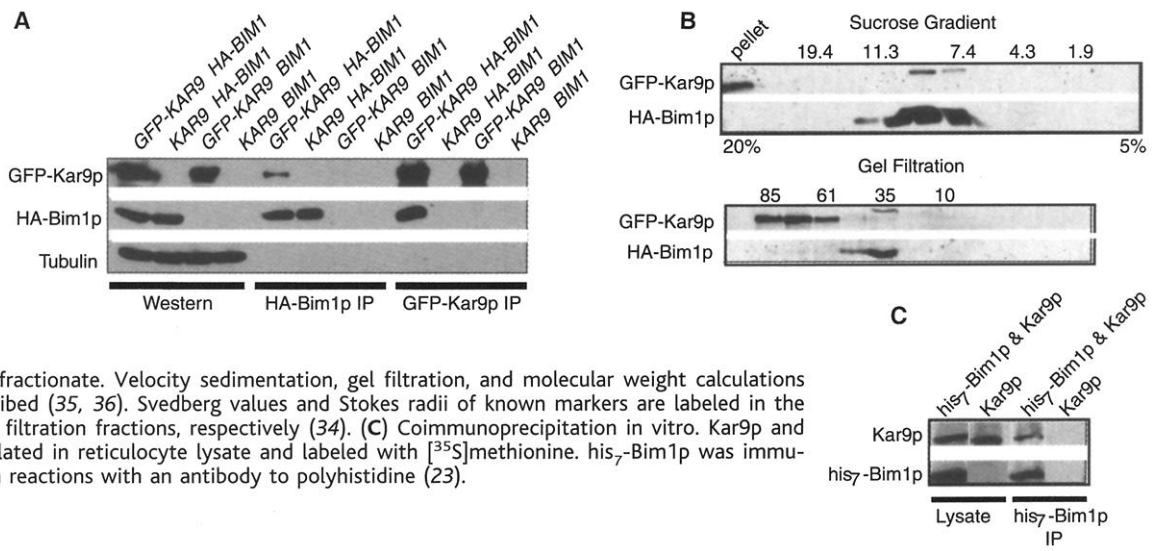

Fig. 3. Kar9p and Bim1p physically interact. (**A**) Coimmunoprecipitation from extracts. Yeast extracts from strains expressing GFP-Kar9p and HA-Bim1p and controls were immunoprecipitated (IP) with antibodies to HA or GFP, and then immunoblotted for GFP-Kar9p, HA-Bim1p, and tubulin (*34*). (**B**) GFP-Kar9p and HA-Bim1p cofractionate. Velocity sedimentation, gel filtration, and molecular weight calculations were performed as described (*35, 36*). Svedberg values and Stokes radii of known markers are labeled in the sucrose gradient and gel filtration fractions, respectively (*34*). (**C**) Coimmunoprecipitation in vitro. Kar9p and his_7-Bim1p were cotranslated in reticulocyte lysate and labeled with [^{35}S]methionine. his_7-Bim1p was immunoprecipitated from both reactions with an antibody to polyhistidine (*23*).

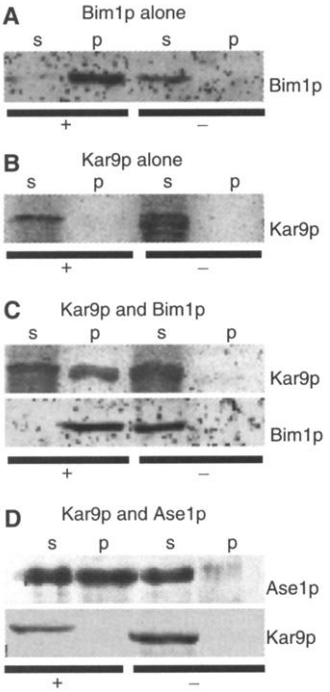

Fig. 4. Bim1p recruits Kar9p onto microtubules in vitro. **(A)** his_7-Bim1p microtubule-binding experiment; **(B)** [^{35}S]Kar9p microtubule-binding experiment; **(C)** Experiment containing both his_7-Bim1p and [^{35}S]Kar9p; **(D)** Experiment containing [^{35}S]Kar9p and recombinant Ase1p. (+) indicates experiments with taxol-stabilized bovine microtubules; (–) indicates experiments without tubulin. s, supernatant; p, pellet. Greater than 80% of the tubulin fractionated into the pellet in the microtubule-binding assays as demonstrated by Coomassie Brilliant Blue stained gels. In the microtubule-binding assays, the concentration of tubulin was 1 μM and the concentration of his_7-Bim1p and Ase1p was 100 nM. Methods of Bim1p purification, Ase1p purification, and the microtubule-binding assay are as described (*23, 37*).

ordinate spindle or centrosome positioning with cell migration. Chromosomal instability, a hallmark of colon cancer, might also be accelerated by loss of the EB1-APC interaction.

Note added in proof: Similar results are reported in two independent studies (*38, 39*).

References and Notes

1. T. J. Mitchison and M. W. Kirschner, *J. Cell Biol.* **101**, 766 (1985).
2. A. A. Hyman, *J. Cell Biol.* **109**, 1185 (1989).
3. M. S. Rhyu and J. A. Knoblich, *Cell* **82**, 523 (1995).
4. M. Snyder, S. Gehrung, B. D. Page, *J. Cell Biol.* **114**, 515 (1991).
5. A. J. Hunt and J. R. McIntosh, *Mol. Biol. Cell* **9**, 2857 (1998).
6. E. Fuchs and Y. Yang, *Cell* **98**, 547 (1999).
7. J. Chant and J. R. Pringle, *Curr. Opin. Genet. Dev.* **1**, 342 (1991).
8. S. L. Shaw *et al.*, *Mol. Biol. Cell* **9**, 1627 (1998).
9. R. H. Gavin, *Int. Rev. Cytol.* **173**, 207 (1997).
10. R. A. Heil-Chapdelaine, N. R. Adames, J. A. Cooper, *J. Cell Biol.* **144**, 809 (1999).
11. S. Busson, D. Dujardin, A. Moreau, J. Dompierre, J. R. DeMay, *Curr. Biol.* **8**, 541 (1998).
12. X. Xiang, C. Roghi, N. R. Morris, *Proc. Natl. Acad. Sci. U.S.A.* **92**, 9890 (1995).
13. P. Gonczy, S. Pihchler, M. Kirkham, A. A. Hyman, *J. Cell Biol.* **147**, 135 (1999).
14. T. DeZwaan, E. Ellingson, D. Pellman, D. M. Roof, *J. Cell Biol.* **138**, 1023 (1997).
15. F. R. Cottingham and M. A. Hoyt, *J. Cell Biol.* **138**, 1041 (1997).
16. R. K. Miller *et al.*, *Mol. Biol. Cell* **9**, 2051 (1998).
17. L. Lee, S. K. Klee, M. Evangelista, C. Boone, D. Pellman, *J. Cell Biol.* **144**, 947 (1999).
18. M. Evangelista *et al.*, *Science* **276**, 118 (1997).
19. R. K. Miller and M. D. Rose, *J. Cell Biol.* **140**, 377 (1998).
20. R. K. Miller, D. Matheos, M. D. Rose, *J. Cell Biol.* **144**, 963 (1999).
21. J. S. Tirnauer, E. O'Toole, L. Berrueta, B. E. Bierer, D. Pellman, *J. Cell Biol.* **145**, 993 (1999).
22. L. Lee, J. Y. Liu, D. Pellman, unpublished data.
23. Supplemental material is available at www.sciencemag.org/feature/data/1047337.shl
24. J. P. Juwana *et al.*, *Int. J. Cancer* **81**, 275 (1999).
25. L. Berrueta *et al.*, *Proc. Natl. Acad. Sci. U.S.A.* **95**, 10596 (1998).
26. H. Imamura *et al.*, *EMBO J.* **16**, 2745 (1997).
27. L. Muhua, N. R. Adames, M. D. Murphy, C. R. Shields, J. A. Cooper, *Nature* **393**, 487 (1998).
28. The delivery of Bim1p to cortical Kar9p binding sites could signal the successful completion of spindle positioning and promote cytokinesis on schedule. However, we found that Kar9p was not required for the cytokinesis checkpoint (L. Lee and D. Pellman, unpublished data).
29. E. E. Morrison, B. N. Wardleworth, J. M. Askham, A. F. Markham, D. M. Meredith, *Oncogene* **17**, 3471 (1998).
30. L.-K. Su *et al.*, *Cancer Res.* **55**, 2972 (1995).
31. G. G. Gundersen and T. A. Cook, *Curr. Opin. Cell Biol.* **11**, 81 (1999).
32. K. Schwartz, K. Richards, D. Botstein, *Mol. Biol. Cell* **8**, 2677 (1997).
33. An astral microtubule was considered correctly oriented if it extended into the bud or mating projection. Analysis was limited to microtubules of length equal to or greater than the shortest distance from the centrosome to the GFP-Kar9p signal. The percentage of preanaphase cells that met the above criteria was 89% in the *BIM1* strain (n = 100) and 8% in the *bim1*Δ strain (n = 228). In α factor–arrested cells, the percentage was 89% in the *BIM1* strain (n = 141) and 27% in the *bim1*Δ strain (n = 321). It is likely that misoriented microtubules in *bim1*Δ cells are misoriented because they fail to interact with Kar9p. If this is the case, then Bim1p is required for microtubule ends to interact with Kar9p in most cells.
34. Cell extracts for Western analysis and immunoprecipitations were prepared by glass bead lysis in a buffer containing 150 mM NaCl, 50 mM Tris (pH 8.0), 1% Nonidet P-40, and protease inhibitors. Antibodies for immunoblotting: HA-Bim1p was detected with 12CA5, GFP-Kar9p was detected with a polyclonal antibody to GFP, and tubulin was detected with a monoclonal antibody to α tubulin.
35. Sucrose gradients (5 to 20%) were made in 50 mM Tris (pH 8.0) and 150 mM NaCl. We loaded 400 μl of low-speed supernatant on top of each 12.5-ml gradient and spun it overnight in a Beckman SW40 Ti at 218,000*g*. The linearity of the gradients was confirmed by refractometry, and Svedberg values were calculated on the basis of globular standards. Gel filtration was performed using a Bio-Rad SE-1000 analytical Gel Filtration column.
36. L. M. Siegel and K. J. Monty, *Biochim. Biophys. Acta* **112**, 346 (1966).
37. K. A. Butner and M. W. Kirschner, *J. Cell Biol.* **115**, 717 (1991).
38. W. S. Korinek, M. J. Copeland, A. Chaudhuri, J. Chant, *Science* **287**, 2257 (2000).
39. R. K. Miller, S.-C. Cheng, M. D. Rose, in preparation.

40. We thank J. DeCaprio, E. Elion, J. Kahana, R. Miller, M. Rose, and P. Silver for reagents, E. Elion, R. Li, T. Look, and M. McLaughlin for comments on the manuscript, J. Chant and M. Rose for communicating results before publication, and B. Bierer and members of the Pellman laboratory for discussions. Supported by grants from NIH [GM55772 to D.P. and KO8 DK02578 to J.S.T.] and a Kimmel Scholar Award to D.P.

23 November 1999; accepted 15 February 2000

Driving AMPA Receptors into Synapses by LTP and CaMKII: Requirement for GluR1 and PDZ Domain Interaction

Yasunori Hayashi,* Song-Hai Shi,* José A. Esteban, Antonella Piccini, Jean-Christophe Poncer,† Roberto Malinow‡

To elucidate mechanisms that control and execute activity-dependent synaptic plasticity, α-amino-3-hydroxy-5-methyl-4-isoxazole propionate receptors (AMPA-Rs) with an electrophysiological tag were expressed in rat hippocampal neurons. Long-term potentiation (LTP) or increased activity of the calcium/calmodulin-dependent protein kinase II (CaMKII) induced delivery of tagged AMPA-Rs into synapses. This effect was not diminished by mutating the CaMKII phosphorylation site on the GluR1 AMPA-R subunit, but was blocked by mutating a predicted PDZ domain interaction site. These results show that LTP and CaMKII activity drive AMPA-Rs to synapses by a mechanism that requires the association between GluR1 and a PDZ domain protein.

Long-term potentiation (LTP) of synaptic transmission is a well-characterized form of activity-dependent plasticity likely to play important roles in learning and memory (*1*). A key mediator of this plasticity is CaMKII, an enzyme that is strongly expressed at excitatory synapses (*2*). Although the cell biological processes underlying this form of plasticity are poorly understood, the trafficking of synaptic receptors appears to play a crucial role (*3*).